

Density-functional study of hydrogen chemisorption on vicinal Si(001) surfaces

E. Pehlke

Physik Department T30, Technische Universität München, D-85747 Garching, Germany

P. Kratzer

Fritz-Haber-Institut der Max-Planck-Gesellschaft, Faradayweg 4-6, D-14195 Berlin-Dahlem, Germany

(Received 19 June 1998)

Relaxed atomic geometries and chemisorption energies have been calculated for the dissociative adsorption of molecular hydrogen on vicinal Si(001) surfaces. We employ density-functional theory, together with a pseudopotential for Si, and apply the generalized gradient approximation by Perdew and Wang to the exchange-correlation functional. We find the double-atomic-height rebonded D_B step, which is known to be stable on the clean surface, to remain stable on partially hydrogen-covered surfaces. The H atoms preferentially bind to the Si atoms at the rebonded step edge, with a chemisorption energy difference with respect to the terrace sites > 0.1 eV. A surface with rebonded single atomic height S_A and S_B steps gives very similar results. The interaction between H-Si-Si-H monohydride units is shown to be unimportant for the calculation of the step-edge hydrogen occupation. Our results confirm the interpretation and results of the recent H_2 adsorption experiments on vicinal Si surfaces by Raschke and Höfer described in the preceding paper.

[S0163-1829(99)13303-4]

I. INTRODUCTION

The interaction of hydrogen with silicon surfaces has become an intensively studied matter. There are important applications in semiconductor technology, such as the passivation of surfaces, etching, and chemical vapor deposition growth.¹⁻³ The attachment of the deposited Si atoms at surface steps is an essential aspect of epitaxial growth.⁴⁻⁸ From the difference in hydrogen chemisorption energy between the adsorption sites on the terraces and at the steps of a vicinal Si(001) surface the equilibrium hydrogen occupation of the various surface sites can be derived. If hydrogen atoms preferentially bind to the step edge, already small hydrogen coverages are sufficient to saturate the Si dangling bonds at the step edge, and thereby to affect the probability of Si atoms to become attached to the step. In this way the kinetics of Si epitaxial growth can be affected by the presence of hydrogen. Of course there are also other mechanisms, like the hydrogen-induced change of the Si surface diffusion coefficient.¹ Furthermore, within the framework of thermodynamic equilibrium theory, the step energies govern the surface morphology on a mesoscopic length scale.⁹⁻¹¹ As step energies depend on hydrogen coverage, the adsorption of hydrogen on the surface could affect step roughness or even surface morphology.¹²

Last but not least, the dissociative adsorption and associative desorption of molecular hydrogen on the Si(001) surface has attracted a great attention, in particular, because adsorption and desorption experiments have led to apparently contradictory results with respect to the adsorption energy barrier. On the one hand, the observed small sticking coefficient suggests a large adsorption energy barrier, while, on the other hand, the kinetic energy distribution of the desorbing hydrogen molecules is nearly thermal, suggesting only a small adsorption energy barrier.^{13,14} Despite intensive research there are still competing explanations. In the dynamical

model by Brenig and co-workers^{15,16} the desorption proceeds from two hydrogen atoms bound to the two Si atoms of a single surface dimer. This hydrogen pairing is corroborated by the observed first-order desorption kinetics of the hydrogen, and the deviations towards second order at very small hydrogen coverage.¹⁷ Brenig's model contains a barrier; the small kinetic energy of the desorbing particles is ascribed to an efficient energy transfer into the Si surface phonon degrees of freedom during the desorption process. However, several quantum-chemical cluster calculations¹⁸⁻²¹ have arrived at distinctly larger barriers than density-functional slab calculations,²²⁻²⁴ and these large desorption energy barriers appear to be at variance with the desorption dynamics sketched above. Thus the authors of these calculations favor models, in which the adsorption on and desorption from surface defects play a major role.²⁵⁻²⁸ On the other hand, Pai and Doren²⁹ obtained barriers from density-functional cluster calculations that are consistent with the prepairing model.

To investigate the role of steps and defects experimentally, Raschke and Höfer³⁰ have studied the adsorption of H_2 on vicinal Si(001) surfaces. For studied miscut angles larger than 2° double atomic height D_B steps prevail on the clean surface.^{10,31} Raschke and Höfer infer from their experimental results that H_2 molecules preferentially adsorb at the step sites. Most importantly, they can distinguish between the contribution of terraces and steps to the H_2 -sticking coefficient. Contrary to the large barrier towards H_2 adsorption on the flat surface and on the terraces, there appears to be only a rather minor (~ 0.09 eV) adsorption energy barrier along the reaction path that leads to dissociative adsorption at the step edge.³² The measured hydrogen step-saturation coverage of about one H atom per (1×1) surface lattice constant a along the step is consistent with a model in which the hydrogen atoms bind to the edge of the double atomic height steps in a local monohydridelike geometry. Furthermore, at

elevated temperatures Raschke and Höfer observe the diffusion of the adsorbed hydrogen atoms from the step onto the terrace. From the measured equilibrium hydrogen coverage on the step edge and on the terrace they deduced a difference between the local chemisorption energies of roughly 0.2 eV by which the hydrogen atoms bind more strongly to the step edge Si atoms.³³

In view of the great importance of H₂/Si(001) as a model system to understand the dynamics of adsorption and desorption, and in view of the conflicting results of quantum-chemical and density-functional theory (DFT) based computations of the adsorption energy barrier of the flat surface, it appears to be quite desirable to calculate the H₂ chemisorption energies and adsorption energy barriers for vicinal surfaces. A successful comparison of DFT results to the new experimental data would lend support to both the interpretation of the experiment and the credibility of the generalized gradient approximation to the exchange-correlation functional used in the DFT calculations.

The purpose of this work is to provide a comprehensive overview over H₂ chemisorption on Si(001) vicinal surfaces: Relaxed geometries and chemisorption energies will be presented for various adsorption sites and step topologies. The adsorption energy barriers on the terrace and at the step edge will be discussed in a forthcoming paper.³²

The organization of the paper is as follows: First, the stable configurations of the clean steps (which are a function of miscut angle) are reviewed in Sec. III A. These structures have already been thoroughly investigated both experimentally^{34–36} and theoretically.^{37–39} However, the stability of these steps in the presence of hydrogen is not *a priori* obvious, and to our knowledge has not been calculated before. Therefore hydrogen adsorption on three different atomic step topologies, which have previously been discussed in context with the clean surface,³⁷ will be considered in Secs. III B–III D. A comparison between these results can lead to a better understanding of the mechanism leading to the different chemisorption energies. Finally, the interaction between neighboring monohydride groups on the surface will be discussed in Sec. III E. A quantitative comparison to Raschke and Höfer's³³ experimental data is given in Sec. III F.

II. COMPUTATIONAL METHOD

The total-energy minimizations and geometry optimizations have been carried out using the electronic-structure code fhi96md (Ref. 40) in a version parallelized for the CRAY T3E architecture. In this code total energies and forces acting on the atoms are calculated within DFT. The generalized gradient approximation (GGA) by Perdew and Wang⁴¹ is applied to the exchange-correlation energy functional. The GGA is known to be distinctly more reliable than the local density approximation (LDA) especially with respect to binding energies, while the LDA has proven insufficient for the calculation of energy barriers of reactions involving hydrogen.^{41–43} Though recently Nachtigall and Jordan²¹ have argued that even the GGA is not sufficiently accurate for the calculation of energy barriers, the use of the GGA is expected to be fully adequate for the less demanding problem of calculating energy differences for hydrogen at-

oms adsorbed on—in our case even chemically rather similar—sites on the Si surface.

The Si atoms are represented by pseudopotentials, which have been constructed according to Hamann's scheme,^{44,45} consistently using the same GGA for the construction of the pseudopotential and the solid state calculations.⁴⁶ For the hydrogen atoms we take the full $1/r$ Coulomb potential.

The electronic wave functions are expanded into plane waves up to a cutoff energy E_{cut} . The integration over the Brillouin zone is replaced by a summation over one or two special \mathbf{k} points.⁴⁷ The \mathbf{k} points are chosen equidistant and aligned along the direction of the step edge. We assume no symmetry restrictions to the atomic geometry during relaxation, the only symmetry exploited in these calculations is time reversal. To give the reader an impression of the residual error due to the finite cutoff energy and \mathbf{k} -point set, we will quote below numerical results at two levels of accuracy: The (30 Ry, 1 \mathbf{k}) data result from geometry relaxation runs using $E_{\text{cut}} = 30$ Ry (408 eV) plane-wave cutoff energy and one special \mathbf{k} point (not the Γ point). Important calculations have been repeated with 50 Ry (680 eV) cutoff energy and 2 \mathbf{k} points, using the frozen geometry from the previous (30 Ry, 1 \mathbf{k}) run. At 50 Ry cutoff energy there are about 153 000 complex plane wave coefficients for every band and \mathbf{k} point.

Total energies are calculated for Si(1 1 1) slabs with a thickness of about six atomic layers, using a supercell that is periodically repeated in all three dimensions. This surface orientation corresponds to a miscut angle of 7.3° in the [110] direction away from (001). On the D_B stepped surface the (1×2) dimerized terraces are four dimers wide, ensuring that we can neglect elastic step-step interactions⁴⁸ when generalizing the results to smaller miscut angles. Furthermore, the large terrace width allows us to distinguish between dimers close to the step edge and those in the center of the terrace. The width of the supercell amounts to $2a$, allowing for one Si-dimer row perpendicular to the step edge. The surface unit cell on the top of the slab contains either a single double atomic height step or a pair of single atomic height steps. The atoms in the bottom two Si layers are fixed at their bulk positions. We use the theoretical equilibrium lattice constant $c = a\sqrt{2} = 5.450$ Å. On the bottom surface the slab is saturated with H atoms in a local dihydride configuration. In case of the clean surface our supercell contains altogether 74 Si atoms and 22 H atoms. All atoms apart from those in the bottom two Si layers and the bottom H termination are allowed to relax by following the computed Hellman-Feynman forces. Residual forces are smaller than 3×10^{-2} eV/Å.

All results quoted below are plain total-energy differences, not corrected for the zero-point energy (ZPE) of the atoms. For the vibration of the free H₂ molecule the ZPE is $\hbar\omega/2 = 0.272$ eV. For hydrogen atoms adsorbed on a Si surface in a monohydridelike configuration the frequency of the Si-H vibrations does not depend much on the details of the configuration.⁴⁹ Results from electron energy loss spectroscopy indicate for Si(001) (2×1) H one stretching mode at 0.260 eV, and two bending modes at 0.0785 eV.⁴⁹ For two adsorbed H atoms this gives a ZPE of 0.417 eV. We neglect changes of the Si phonon frequencies due to hydrogen adsorption. Within this approximation the ZPE correction leads to only a rigid shift of all chemisorption energies by 0.145

eV. For deuterium this shift would be smaller by about a factor of $1/\sqrt{2}$. Differences between chemisorption energies are not affected by the ZPE correction, i.e., they can be directly read from the tables below.

III. RESULTS AND DISCUSSION

In the following we present our DFT results and discuss the implications for the thermodynamics of partially H-covered vicinal Si surfaces. First, however, we briefly summarize our results for the step energies and relaxed geometries of the clean surface. In the subsequent Secs. III B–III D the chemisorption energies will always refer to the respective clean surface plus a hydrogen molecule at rest far away from the surface as energy zero. Thus, in order to find out which step topology is stable (at zero temperature), one first has to add the respective step energies from Sec. III A to the chemisorption energies before comparing the total energies of different step topologies with each other. As explained in the previous Sec. II, we expect the contributions from the zero point energy to cancel out when a total energy difference between rather similar, mono-hydride like configurations is calculated.

It should be noted here that the probability of observing a certain type of step (e.g., S_A - S_B or D_B) along a step edge at some finite temperature cannot be simply inferred from the respective step energies per unit step length. The step energy difference per unit length has to be multiplied with an appropriate coherence length first (which describes the average extent of a kink-free part of the step) in order to obtain an excitation energy that makes sense to enter in a Boltzmann factor.⁵⁰

Our objective is to characterize the lowest energy configurations for two H atoms adsorbed on the vicinal Si surface. The pairing energy for two hydrogen atoms on the Si(001) surface has been measured by Höfer, Li, and Heinz¹⁷ to be about 0.25 eV, which is close to the DFT result by Northrup.⁵¹ This value is larger than the chemisorption energy difference between typical adsorption sites. Therefore we have restricted ourselves to configurations with two hydrogen atoms adsorbed on the same silicon dimer, i.e., we have only considered the H-paired configurations. Of course the unpaired H configurations will become important when comparing to an experiment carried out at high temperature and low H coverage, where entropy plays an essential role. We postpone this issue until Sec. III F.

A. Atomic geometry of clean vicinal Si(001) surfaces

A characteristic feature of the flat Si(001) surface are the Si dimers.⁵² By forming these dimers the density of dangling bonds is halved in comparison to the bulk terminated surface. The Si dimers are not parallel to the surface.^{53–58} In our calculation the buckling angle amounts to about 19° on the $p(2\times 2)$ dimerized (001) terrace, in agreement with experiment^{57,58} and previous DFT work.^{59,60} The energy lowering is driven by the rehybridization of the sp^3 orbitals of the Si atom that relaxes towards the bulk: Its bonding geometry becomes more planar, and therefore the bonding orbitals become more sp^2 like, while the dangling bond gains more p character and becomes unoccupied. The dangling bond of the other Si dimer atom that relaxes outwards is fully occupied.

This implies that the π bond between the Si atoms of the symmetric dimer is partially destroyed by buckling, however, in case of Si the energy gain due to the rehybridization mechanism obviously over-compensates this energy cost. The buckling of the surface dimers is accompanied by a change from a metallic to a semiconducting electronic surface band structure.⁶¹ Due to elastical coupling via the atoms in the second and deeper layers the buckling angle alternates along the dimer row. The lowest-energy reconstruction is $p(2\times 2)$, or, even slightly lower, $c(4\times 2)$, but the energy difference between these reconstructions is so small that it is irrelevant for our purpose.⁶⁰ Thus we assume the $p(2\times 2)$ reconstruction on the terraces, which allows us to keep the supercell small.

The vicinal Si(001) surface can be imagined as a staircase with (001) terraces separated by steps. At small miscut angles less than $\sim 1^\circ$, the vicinal surface consists of alternating single atomic height S_A and S_B steps,¹⁰ and, consequently, the direction of dimerization rotates by 90° on successive terraces. There occurs a presumably gradual transition initiating at about 1° to 2° , driven by elastic step-step interactions, and at large miscut angles the surface becomes more and more single-domain with predominantly double atomic height steps.^{10,62,63,31,64} These steps have been identified both experimentally and theoretically to display the rebonded D_B geometry, with threefold coordinated Si atoms at the step edge.^{37,34,35}

We use the clean Si surface as the energy reference for the chemisorption energies discussed below. Therefore we have computed the relaxed geometries and total energies for the three step configurations displayed in Fig. 1. Our results turned out to be in agreement with previous DFT studies of steps on the Si(001) surface.^{38,39} However, note that the choice of, e.g., the plane-wave cutoff energy is determined by the requirement to accurately describe hydrogen-containing systems, it is not adapted to the calculation of Si step energies, for which a much smaller cutoff would be sufficient. However, to obtain accurate step interaction energies, thicker Si slabs would be necessary.⁴⁸

An S_A - S_B step pair is displayed in Fig. 1(a). The (1×2) and (2×1) terraces are both $2a$ wide. The bonds between the two rebonded Si atoms and the neighboring step-edge atom are highly strained, they are 4% and 7% longer than the bulk Si-Si bond. The Si surface dimer bonds are 0–2.4% shorter than the bulk bond length, and the buckling angle varies between 18° and 15° , i.e., the buckling is partially suppressed close to the steps. The electronic structure is characterized by occupied dangling bonds at the Si dimer and step edge atoms that have relaxed outwards. The rehybridization mechanism works for the rebonded Si atom at the step edge in the same way as for the Si dimer atoms, it results in a height difference between neighboring rebonded step edge atoms of 0.7 Å. This is close to the result by Bogusławski *et al.*³⁸ of 0.58 Å.

The double atomic height nonrebonded D_B' and rebonded D_B steps are shown in Figs. 1(b) and 1(c), respectively. The nonrebonded geometry corresponds to a double layer of Si, which is terminated at the step edge. There are no rebonded Si atoms with highly strained bonds, thus the elastic interaction of the D_B' steps is small. Among the step structures considered, this one has the smallest strain field on the ter-

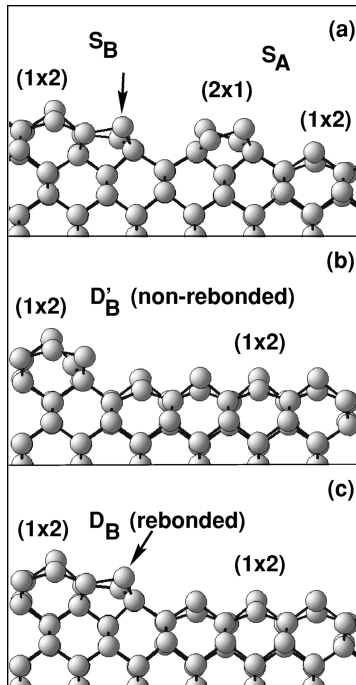


FIG. 1. Relaxed atomic geometry of single and double atomic height steps on the Si(001) surface. The orientation of the vicinal surface is (1 1 1), corresponding to a miscut angle of $\Theta = 7.3^\circ$. A side view along the $[1\bar{1}0]$ direction parallel to the step edge is shown. (a) Pair of single atomic height S_A and S_B steps. Terraces are alternate (1×2) and (2×1) dimerized. (b) Nonrebonded double atomic height D'_B step. (c) Rebonded double atomic height D_B step. In (a) and (c) the rebonded Si atoms at the S_B and D_B step edges are denoted by arrows.

faces. Therefore the dimers in the middle of the (1×2) terrace between the D'_B steps most closely resemble the dimers on the flat surface. The buckling angle of the surface dimers varies between 18° close to the step and 19° in the middle of the terrace. Again, rehybridization results in a pronounced buckling at the step edge. However, there is an important difference between the rebonded configurations (a) and (c) and the nonrebonded D'_B step: We find the Si-Si bond between the two Si atoms on the upper terrace closest to the step edge to be contracted by 3%, which indicates a strong additional π bond between these atoms.³⁹

It was already pointed out by Chadi³⁷ that the nonrebonded D'_B step is not the lowest-energy configuration. The number of dangling bonds can be lowered by adding an extra ‘rebonded’ Si atom to the D'_B step edge. The rebonded D_B structure is shown in Fig. 1(c), it can be described as a collapsed S_A - S_B step pair, with the width of the (2×1) terrace shrunk to zero. Similar to the S_B step, the bonds between the two rebonded Si atoms and the neighboring step-edge atoms are highly strained, 4% and 7.7% longer than a Si-Si bulk bond (4.7%–6.6% in Ref. 39). The force dipole from these bonds induces a strain field and results in a considerable step-step interaction. We find a variation of the dimer buckling angle between 18° in the middle of the terrace and 16° on the lower terrace close to the step edge. The dimer bond lengths vary between 0% and 2% contraction. Compared to the S_A - S_B step pair we find the D_B step to be ~ 0.02 eV per step length $2a$ lower in energy. However, note that this en-

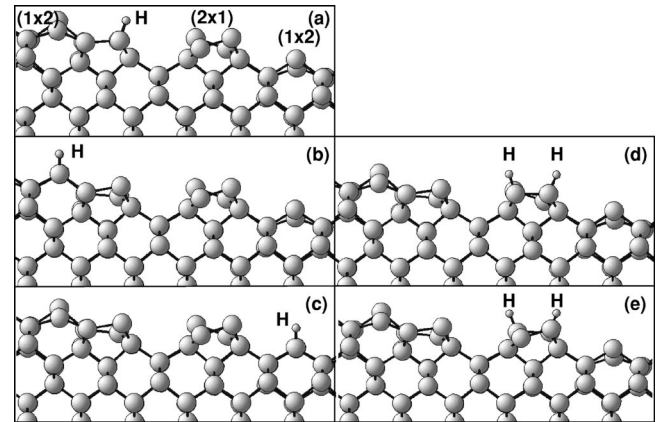


FIG. 2. Relaxed atomic geometries for two hydrogen atoms adsorbed at different sites on a Si(1 1 1) surface with single atomic height steps. Side view along the $[1\bar{1}0]$ direction as in Fig. 1. In (a)–(c) the hydrogen atoms are arranged in a row parallel to $[1\bar{1}0]$, thus only the atom in the front is visible. (a) Two hydrogen atoms adsorbed at the S_B step edge in a local monohydride configuration. (b) Two hydrogen atoms adsorbed at the Si dimer on the upper (1×2) terrace close to the S_B step. (c) Two hydrogen atoms adsorbed at the Si dimer on the lower (1×2) terrace close to the S_A step. (d) and (e) Two hydrogen atoms adsorbed at a dimer on the (2×1) terrace.

ergy difference is smaller than our rough error estimate of ~ 0.05 eV, thus the agreement with observation is partially fortuitous.

To compare the energy of the rebonded and nonrebonded double atomic height steps we have calculated the Si chemical potential by using the same supercell and convergence parameters as above and adding four Si atoms to the bulk of the slab while keeping the top and bottom surface structures intact. In agreement with previous work we find the nonrebonded D'_B step to be energetically unfavorable. However, our energy difference of 0.13 eV/ a is larger than Oshiyama’s³⁹ result of 0.06 eV/ a . This may be connected to the fact that we observe a more pronounced relaxation of the atoms at the D_B step edge, a height difference of the rebonded atoms of 0.6 Å in contrast to the much smaller value of 0.17 Å in Ref. 39. We think that our large step-edge relaxation is corroborated by the similarity between the D_B and S_B steps together with the fact that we agree with Bogusławski *et al.*³⁸ with respect to the pronounced relaxation of the S_B step.

In view of the smaller number of dangling bonds at the D_B step the energy lowering with respect to the D'_B step appears to be rather small. This can be explained by the extra π bonds stabilizing the D'_B step, and the large Si-Si bond strain destabilizing the D_B step. Both effects diminish the energy difference suggested by simple bond counting.

B. Hydrogen adsorbed on surfaces with S_A - S_B steps

The relaxed geometries for two hydrogen atoms adsorbed on a surface dimer or at the two rebonded Si atoms are shown in Fig. 2 for a vicinal surface with single atomic height steps. In (a) the two H atoms saturate the dangling bonds of the rebonded Si atom at the S_B step edge. Therefore there is no driving force towards buckling anymore and the

TABLE I. Chemisorption energy for two H atoms adsorbed on a Si(111) surface with single atomic height steps. The respective adsorption geometries are shown in Fig. 2. The energies refer to a free H₂ molecule at rest far away from an S_A-S_B vicinal surface, the ZPE correction is not included. The data in parentheses have been calculated at 30 Ry cutoff energy with one special **k** point. The final energies have been calculated at 50 Ry, using two special **k** points in the irreducible part of the Brillouin zone, and taking the frozen geometries from the 30 Ry, one **k**-point run.

	Adsorption site	Chemisorption energy (eV)
(a)	H at rebonded S _B	-2.10 (-2.13)
(b)	H on (1×2) terrace	-1.78 (-1.85)
(c)	H on (1×2) terrace	-1.96 (-2.01)
(d)	H on (2×1) terrace	-1.90 (-1.91)
(e)	H on (2×1) terrace	-1.89 (-1.89)

two rebonded Si atoms become nearly equivalent. The Si-Si bond between the Si step edge atom and its neighbor on the upper terrace is strained by about 5% compared to the Si-Si bulk bond length. This is almost identical to the average strain of these bonds on the clean surface, i.e., the step interaction will not be much affected by adsorption.

On the whole, the geometry changes upon hydrogen adsorption are quite local. As can be seen in (b)–(e), the H-saturated dimers are parallel to the (001) surface. The respective Si-Si dimer bond lengths are 1.6%–2.6% larger than the Si-Si bulk bond length. The Si-H bond length amounts to 1.51 Å.

The various chemisorption energies are summarized in Table I. We find the adsorption at the rebonded S_B step-edge atom to be energetically favored, with an energy difference of at least 0.14 eV with respect to adsorption on terrace sites. Note that for a comparison of the total energies of the final state configurations after hydrogen adsorption on, e.g., the S_A-S_B and the D_B stepped surface, the step energy difference of 0.02 eV per step length $2a$ has to be added to the numbers given in Table I.

C. Hydrogen adsorbed on surfaces with D_B steps

The relaxed geometries for two hydrogen atoms adsorbed on a vicinal silicon surface with D_B steps are shown in Fig. 3. The observed relaxations as well as the chemisorption energies summarized in Table II are similar to the results we found for the single atomic height steps.

In Fig. 3(a) the two hydrogen atoms saturate the dangling bonds of the two rebonded Si atoms at the step edge. Consequently, the buckling of the step-edge atoms disappears. The strain of the bond to the neighboring Si atom on the upper terrace amounts to 5.3% elongation, close to the average strain of these bonds on the clean surface. The buckling of the surface dimers on the (1×2) terrace remains almost unaffected by hydrogen adsorption at the step edge. Hydrogen adsorption on the terrace [Fig. 3(b)–3(e)] leads to local monohydride configurations. The H-saturated Si-dimer debuckles, and the Si-Si dimer bond length expands by 1.9%–2.5%.

From the chemisorption energies in Table II we read that the H atoms preferentially adsorb on the rebonded Si atom at

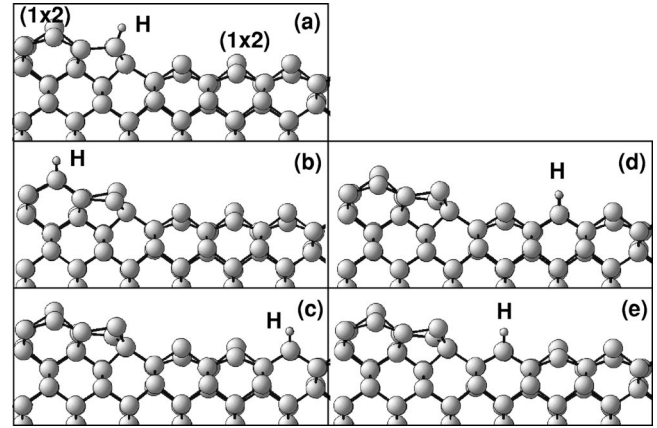


FIG. 3. Relaxed atomic geometries for two hydrogen atoms adsorbed at different sites on a Si(111) surface with D_B steps. Side view along the [1 $\bar{1}$ 0] direction as in Fig. 1. The hydrogen atoms are arranged in a row parallel to [1 $\bar{1}$ 0], thus only the atom in the front is visible. (a) Two hydrogen atoms adsorbed at the D_B step edge in a local monohydride configuration. (b)–(e) Two hydrogen atoms adsorbed at the various inequivalent Si dimers on the (1×2) terrace.

the D_B step edge. In comparison to the adsorption sites on the terrace the step is energetically favorable by at least 0.12 eV. We speculate that this may be due to both the different elastic relaxation energies at the step edge and on the terrace and some residual π bond between the surface dimer atoms as opposed to the step edge atoms. A rigorous quantitative analysis of the energy contributed by the different possible mechanisms, however, is beyond the scope of this paper.

Comparing the total energies for hydrogen attached to the D_B and S_A-S_B step edge we find no significant energy difference within the accuracy of our approach.

We have repeated our calculations for a smaller supercell describing a Si(117) surface with D_B steps, which has two Si dimers per (1×2) terrace. The chemisorption energies are summarized in Table III. They compare very well with the values for the Si(111) surface in Table II, i.e., we do not find any pronounced effect of miscut angle on chemisorption energies. This lends support to the use of the smaller, and

TABLE II. Chemisorption energy for two H atoms adsorbed on a Si(111) surface with double atomic height D_B steps. The respective adsorption geometries are shown in Fig. 3. The energies refer to a free H₂ molecule at rest far away from a clean D_B-stepped vicinal surface, the ZPE correction is not included. The data in parentheses have been calculated at 30 Ry cutoff energy with one special **k** point. The final energies have been calculated at 50 Ry, using two special **k** points in the irreducible part of the Brillouin zone, and taking the frozen geometries from the 30 Ry, one **k**-point run.

	Adsorption site	Chemisorption energy (eV)
(a)	H at rebonded D _B	-2.09 (-2.11)
(b)	H on (1×2) terrace, pos. 1	-1.77 (-1.82)
(c)	H on (1×2) terrace, pos. 2	-1.92 (-1.95)
(d)	H on (1×2) terrace, pos. 3	-1.97 (-2.00)
(e)	H on (1×2) terrace, pos. 4	-1.97 (-2.01)

TABLE III. Chemisorption energy for two H atoms adsorbed on a Si(117) surface with double atomic height D_B steps. The energies refer to a free H_2 molecule at rest far away from a clean D_B -stepped Si(117) surface, the ZPE correction is not included. The data have been calculated at 50 Ry cutoff energy with two special \mathbf{k} points.

Adsorption site	Chemisorption energy (eV)
H at rebonded D_B	-2.07
H on (1×2) terrace, pos. 1	-1.75
H on (1×2) terrace, pos. 4	-1.93

thus computationally more convenient, Si(117) supercell for the calculation of, e.g., the hydrogen adsorption barriers on vicinal Si(001) surfaces.

A further issue that needs to be investigated is the existence of different surface geometries corresponding to local minima of the total energy in configuration space. For this purpose we have taken the configuration displayed in Fig. 3(d) and flipped the buckling angle of all dimers to the left hand side or to the right hand side of the monohydride group up to the neighboring step edge from $+\Theta$ to $-\Theta$, and vice versa. Then these starting configurations were relaxed in the standard way. In this way we found new stable configurations, which, however, are all energetically degenerate within the accuracy of our approach. At room temperature and above, the dimers flip rapidly between the two stable orientations.

The large strain of the bond between the D_B step-edge atom (i.e., the rebonded Si atom) and the neighboring Si atom on the upper terrace supports the speculation that this bond could break upon hydrogen adsorption and that a local dihydride group might form at the position of the former step edge atom. Therefore we have calculated the total energy of the relaxed dihydride geometry on a Si(117) surface, however, we found it to be energetically distinctly unfavorable. The respective hydrogen chemisorption energy amounts to only -0.87 eV.

D. Hydrogen adsorbed on surfaces with nonrebonded D'_B steps

Relaxed geometries for two hydrogen atoms adsorbed on a Si(111) surface with nonrebonded D'_B steps are displayed in Fig. 4, and the respective chemisorption energies are given in Table IV. Interestingly, the nonrebonded step behaves totally different from the rebonded steps discussed in the previous sections. In particular, the hydrogen adsorption at the step edge [i.e., on the adsorption sites shown in (a) and (b) of Fig. 4] is distinctly disfavored. We attribute this to the breaking of the strong π bonds between the step edge Si atom and the neighboring Si surface-dimer atom on the upper terrace. This bond is contracted by 3% on the clean surface and in the configurations (c)–(f), while this contraction disappears upon hydrogen adsorption on either of the two sites shown in Figs. 4(a) and 4(b).

On the whole, the absolute values of the chemisorption energies are smaller on the D'_B stepped surface than on the D_B stepped surface. This is also true for another possible hydrogen-adsorption configuration not included in Table IV: The two H atoms can bind to the Si atom at the D'_B step edge

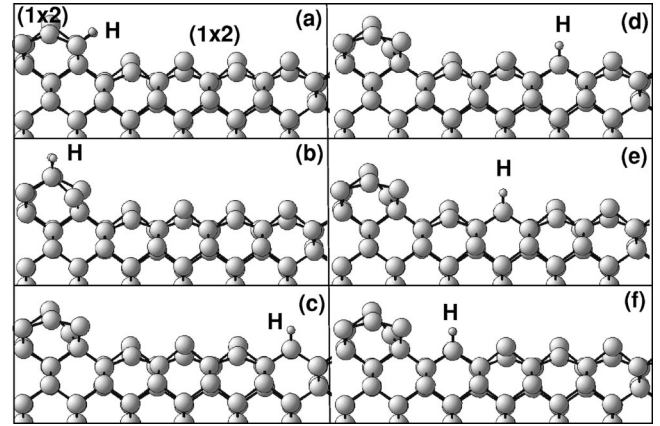


FIG. 4. Relaxed atomic geometries for two hydrogen atoms adsorbed at different sites on a Si(111) surface with nonrebonded D'_B steps. Side view along the $[1\bar{1}0]$ direction as in Fig. 1. The hydrogen atoms are arranged in a row parallel to $[1\bar{1}0]$, thus only the atom in the front is visible. (a) Two hydrogen atoms adsorbed at the D'_B step edge in a local monohydride configuration. (b)–(f) Two hydrogen atoms adsorbed on the various inequivalent Si dimers on the (1×2) terrace.

[Fig. 4(a)] and the neighboring Si-dimer atom [Fig. 4(b)]. For this configuration we estimate⁶⁵ the chemisorption energy to be about -1.78 eV. Together with the fact that already the clean D'_B surface is energetically unfavorable we conclude, that the D'_B step configuration is unstable also after hydrogen adsorption. This holds true unless the hydrogen coverage becomes so large that the hydrogen atoms cannot be accommodated anymore on the D_B stepped surface. Our conclusion is that after adsorption of two hydrogen atoms on a vicinal Si surface the most stable, i.e., lowest energy, configurations consist of the two H atoms bound to either the rebonded S_B or the rebonded D_B step edge.

E. Partially hydrogen-covered surfaces

Next we consider finite hydrogen coverage and interaction effects between neighboring mono-hydride H-Si-Si-H groups on the surface. This will allow us to investigate a possible tendency towards hydrogen island formation, and the energetical competition of such islands, acting as hydro-

TABLE IV. Chemisorption energy for two H atoms adsorbed on a Si(111) surface with nonrebonded D'_B steps. The respective adsorption geometries are shown in Fig. 4. The energies refer to a free H_2 molecule at rest far away from a vicinal Si surface with nonrebonded D'_B steps. The ZPE correction is not included. The calculations have been carried out at 30 Ry, with one special \mathbf{k} point.

	Adsorption site	Chemisorption energy (eV)
(a)	H at nonrebonded D'_B	-1.53
(b)	H on (1×2) terrace, pos. 1	-1.27
(c)	H on (1×2) terrace, pos. 2	-1.93
(d)	H on (1×2) terrace, pos. 3	-1.93
(e)	H on (1×2) terrace, pos. 4	-1.93
(f)	H on (1×2) terrace, pos. 5	-2.02

gen sinks, with the step-edge adsorption sites discussed in the previous sections. To gain further principal insight into the energetics of hydrogen adsorption, we consider both the rebonded D_B and the nonrebonded D'_B step. In this section we still assume the limit of large pairing energy, i.e., the H atoms are assumed to always form complete H-Si-Si-H groups.

For the description of our approach we will restrict ourselves to the rebonded D_B step. The different adsorption sites are enumerated from 0 to 4 as in Table II, and the index 0 denotes the two rebonded Si atoms at the step edge. The H_2 chemisorption energies ϵ_i are taken from the (30 Ry cutoff energy, 1 \mathbf{k} point) results in Table II. This has been done for the sake of a simple comparison to the results for the D'_B step, for which only (30 Ry cutoff energy, 1 \mathbf{k} point) results are available, and for the sake of less expensive *ab initio* calculations. The numbers $n_i, i=0, \dots, 4$, can take the values 0 or 1, with 0 denoting a clean Si surface dimer, and 1 denoting a Si surface dimer with two adsorbed H atoms. We assume the following nearest-neighbor-interaction Hamiltonian to describe the total chemisorption energy (take index 5 to be identical to index 0):

$$H^{(D_B)} = \sum_{i=0}^4 n_i \epsilon_i^{(D_B)} + n_i n_{i+1} w_i^{(D_B)}. \quad (1)$$

As a further approximation we assume the interaction parameters w_i to be equal on the terrace, i.e., $w_1(D_B) = w_2(D_B) = w_3(D_B)$. Effects omitted in this Hamiltonian are (i) the breaking up of H-Si-Si-H pairs into single adsorbed H atoms, (ii) the excitation of the D_B step into S_A - S_B step pairs, and (iii) any effect connected with the configurational entropy due to dimer flips. The three independent interaction parameters w_i have been determined within DFT (at 30 Ry cutoff energy, with 1 \mathbf{k} point), by calculating two geometries with four adsorbed H atoms and the fully H-covered surface. The results for the rebonded D_B step are: $w_0(D_B) = -0.14$ eV, $w_1(D_B) = -0.04$ eV, $w_4(D_B) = -0.009$ eV, and similar calculations for the nonrebonded D'_B step yield: $w_0(D'_B) = -0.75$ eV, $w_1(D'_B) = -0.07$ eV, $w_5(D'_B) = -0.007$ eV. Obviously, the nearest-neighbor interaction is attractive. We attribute it mostly to elastic interaction via the second and deeper layer Si atoms. The extraordinarily large value of $|w_0(D'_B)|$ accounts for the fact that two Si-Si π bonds have already been broken by the first H pair [configurations Figs. 4(a) and 4(b)], thereby favoring the adsorption of the second H-atom pair on the neighboring Si atoms.

Interesting quantities that can easily be calculated from Eq. (1) are the chemisorption “hole” energies, i.e., the chemisorption energy of the last H_2 molecule that is finally completing the full coverage of 1 ML. We label the adsorption sites in analogy to Figs. 3 and 4; to obtain the initial configuration before adsorption just invert the surface H occupation (i.e., every Si dangling bond becomes H covered, apart from those two Si dangling bonds that are saturated by H atoms in the respective panel of Figs. 3 or 4). The chemisorption “hole” energies are summarized in Tables V and VI for D_B and D'_B stepped surfaces, respectively. The accuracy of our model Hamiltonian is demonstrated by the good agreement with two DFT test calculations, in which the

TABLE V. Chemisorption “hole” energy for an almost fully hydrogen-covered Si(1 1 1) surface with D_B steps. The energies have been derived from the model Hamiltonian in Eq. (1). For comparison, the energy values in parentheses are from *ab initio* total-energy calculations (30 Ry cutoff energy, 1 \mathbf{k} point). For the meaning of the labels denoting the position of the hole see Fig. 3.

	Adsorption site	Chemisorption energy (eV)
(a)	rebonded D_B step edge	-2.26 (-2.25)
(b)	(1×2) terrace, pos. 1	-2.00
(c)	(1×2) terrace, pos. 2	-2.03
(d)	(1×2) terrace, pos. 3	-2.08 (-2.07)
(e)	(1×2) terrace, pos. 4	-2.06

atomic geometries have been fully relaxed. Contrary to adsorption on the clean surfaces studied above, we find the rebonded and nonrebonded step configurations to behave very similar in case of the “hole” energies. In particular, for both steps the absolute value of the chemisorption energy takes its maximum for adsorption at the step edge. Furthermore, the chemisorption energies on the terraces in Tables V and VI are all quite similar and below (i.e., more negative than) the values for the clean surfaces. This simplicity is due to two reasons: First, the π bond breaking at the D'_B step does not play a role for the hole energies. Second, there is an elastic coupling between the relaxation of the buckled dimers on the surface and the step edge atoms on the clean surface, which apparently becomes less important when the Si atoms are H covered and the surface Si atoms are not buckled any more. The hydrogen adsorption into the hole configuration is more exothermic than the adsorption on the clean surface due to the different elastic interactions: The dimer buckling on the clean surface tends to stabilize the buckled dimer and thus to destabilize the symmetric dimer of the local monohydride group. Our results are compatible with the energy difference of 0.05 eV/dimer between the asymmetric $p(2 \times 1)$ and the $p(2 \times 2)$ reconstruction of the Si(001) surface calculated by Ramstad, Brocks, and Kelly.⁶⁰

Up to this point we have focused on the chemisorption energies as a function of the different adsorption sites, and therefore it was sufficient to consider only a single dimer string. In the following we will briefly discuss the “thermodynamic ground state” of the whole surface as a function of hydrogen coverage. This means that, while we still stick to

TABLE VI. Chemisorption “hole” energy for an almost fully hydrogen-covered Si(1 1 1) surface with nonrebonded D'_B steps. The energies have been derived from a model Hamiltonian similar to Eq. (1). For the meaning of the labels denoting the position of the hole see Fig. 4.

	Adsorption site	Chemisorption energy (eV)
(a)	nonrebonded D'_B step edge	-2.28
(b)	(1×2) terrace, pos. 1	-2.09
(c)	(1×2) terrace, pos. 2	-2.07
(d)	(1×2) terrace, pos. 3	-2.07
(e)	(1×2) terrace, pos. 4	-2.07
(f)	(1×2) terrace, pos. 5	-2.10

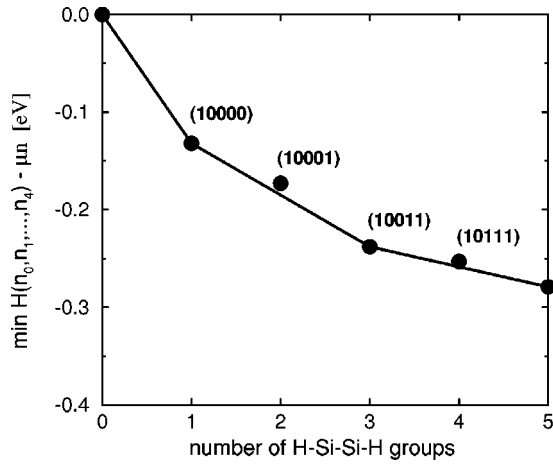


FIG. 5. The dots represent the minimum energy $\min[H(n_0, n_1, \dots, n_4)] - \mu n$ with respect to all configurations (n_0, n_1, \dots, n_4) at fixed n versus the number of H-Si-Si-H groups $n = \sum_{i=0}^4 n_i$, for a Si(1 1 1) surface with D_B steps. The labels denote the lowest-energy configurations. A chemical potential term μn has been subtracted for convenience, with μ chosen equal to the average single-particle chemisorption energy of -1.98 eV. The model Hamiltonian H from Eq. (1) is used together with the *ab initio* energy parameters calculated with 1 \mathbf{k} point at 30 Ry cutoff energy. The full line is the convex hull, which represents the thermodynamic ground-state energy (for temperature $T \rightarrow 0$ K) as a function of n .

the simple Hamiltonian in Eq. (1) to describe the energy of every single dimer row on the D_B stepped surface, we additionally allow for the exchange of hydrogen atom pairs between adsorption sites on different dimer rows. In this way chemisorption configurations with inhomogeneous hydrogen coverage are included in the competition for the lowest total energy. In Fig. 5 the minimum of the energy given by Eq. (1) with respect to all configurations (n_0, n_1, \dots, n_4) , $n_i = 0$ or 1, is plotted versus the number of H-Si-Si-H pairs $n = n_0 + \dots + n_4$. The full line denotes the convex hull and represents the lowest possible energy as a function of n , also accounting for the simultaneous occurrence of different chemisorption configurations on the surface. Figure 5 leads us to the important conclusion that the vicinal surface where all the dangling bonds of the rebonded Si atoms at the D_B step edge are saturated by H atoms [configuration $(n_0, n_1, \dots, n_4) = (1, 0, 0, 0, 0)$] in fact represents the ground state at this certain coverage [i.e., $\Theta = 1/5$ for the Si(1 1 1) surface]. Obviously, the interaction included in Eq. (1) is too weak to stabilize any other state with hydrogen ‘‘islands’’ on the terrace.

In Fig. 6 the lowest energy configurations are shown for the two situations when one or two H-Si-Si-H groups are displaced from the D_B step edge onto the terrace. In (a) the hydrogen group is forced to remain on its dimer string, thus the energy difference can be immediately read from Table II to be equal to 0.10 eV (here we consistently use the results for 30 Ry, 1 \mathbf{k} point; for 50 Ry, 2 \mathbf{k} points the energy difference would amount to 0.12 eV). The energy difference becomes slightly smaller, 0.09 eV, for the configuration displayed in (b), when the hydrogen atoms are transferred onto another dimer string. Finally, when two hydrogen groups are displaced as shown in (c), the energy difference amounts to 0.16 eV.

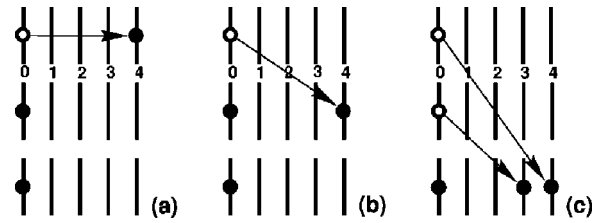


FIG. 6. Metastable configurations for hydrogen adsorbed on a Si(1 1 1) surface with D_B steps and hydrogen coverage $1/5$. The Si surface dimers and the step-edge atoms are denoted by lines. On the terrace the dimers arrange in dimer strings. The open and filled circles denote the positions of the monohydride H-Si-Si-H groups in the ground-state and in the excited-state configuration, respectively. (a) One monohydride group displaced from the step edge onto the terrace within one dimer row. (b) One monohydride group displaced from the step edge onto a terrace site of another dimer row. (c) Two monohydride groups displaced onto another single dimer row.

F. Thermodynamics at low hydrogen coverage

In this section we will present a comparison between our *ab initio* results and the experimental hydrogen adsorption data by Raschke and Höfer described in the preceding paper.³³ They have saturated the D_B step edges of vicinal Si(001) surfaces miscut by 2.5° and 5.5° towards the [110] direction with molecular hydrogen at a surface temperature, which is sufficiently low to suppress the diffusion of the hydrogen atoms onto the terrace. This nonequilibrium configuration can be prepared, because there is a considerable energy barrier towards the dissociative adsorption of the H_2 molecules onto the flat surface or the terrace, while the adsorption-energy barrier at the step edge is very small.^{30,32} At temperatures of 618–680 K partial thermal equilibrium between the adsorption sites at the step and on the terrace is established. After equilibration the configuration is frozen in by rapidly cooling down the sample, and the residual hydrogen coverage at the D_B step-edge site is measured. This is accomplished by determining the amount of hydrogen, expressed as a change of coverage $\Delta\Theta$, necessary to saturate the depleted Si step-edge dangling bonds again. The resulting step-edge H-occupation probability $p_0 = 1 - \Delta\Theta/\Theta_{\text{step}}^{\text{sat}}$, based on the experimental step-edge H-saturation coverage $\Theta_{\text{step}}^{\text{sat}}$, is denoted by the filled circles and the square in Figs. 7 and 8.

To compare to experiment we generalize the Hamiltonian in Eq. (1) from the Si(1 1 1) surface with $N=4$ Si dimers per terrace to D_B -stepped vicinal surfaces with smaller miscut angle and $N > 4$ dimers per terrace. This is done by simply replicating the energy corresponding to configuration (c) on the D_B stepped surface (see Fig. 3) together with the interaction parameter $w_i(D_B)$, which is assumed to be constant on the terrace. The configuration (c) was chosen, because its chemisorption energy is closest to the chemisorption energy on the terraces bounded by D_B' steps. As already noted above, the strain field of the nonrebonded D_B' step is distinctly weaker than that of the rebonded D_B step. Therefore the terraces on the D_B' stepped surface resemble the flat surface (or, equivalently, the middle part of a wide terrace) more closely than any of the other configurations. For the miscut angles 5.4° and 2.45° , corresponding to $N=6$ and

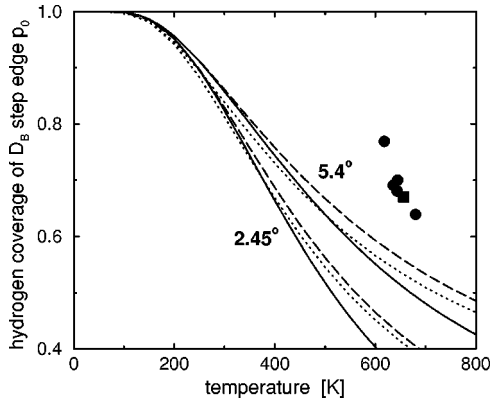


FIG. 7. Probability p_0 , that the Si dangling bond at the D_B step edge is saturated with a hydrogen atom, versus the surface temperature for two vicinal surfaces with miscut angles of 2.45° and 5.4° . The total hydrogen coverage amounts to two hydrogen atoms per dimer string, i.e., it has been chosen equal to $1/(N+1)$ independent of temperature. Different line styles are used to distinguish among the various approximations. Dotted line: Hamiltonian, Eq. (1), including the nearest-neighbor interaction term. Dashed line: Same Hamiltonian, but all interactions w_i set to zero. Full line: Hamiltonian, Eq. (2), with pairing energy $\epsilon_{\text{pair}}=0.25$ eV for all sites. The symbols denote experimental data by Raschke and Höfer for vicinal surfaces with a miscut angle of 2.5° (circles) and 5.5° (square).

$N=15$ dimers per terrace, we have calculated the step-edge occupation probability $p_0=\langle n_0 \rangle$ at fixed hydrogen coverage $\Theta=1/(N+1)$ as a function of surface temperature within the grand canonical ensemble, see the dotted line in Fig. 7. At this small hydrogen coverage the interaction term in the Hamiltonian (1) does not play any important role, as can be judged by comparison to the dashed line in Fig. 7, which was calculated in exactly the same way, but with all interaction parameters w_i set to zero.

However, it is well known¹⁷ that at small hydrogen coverage configurational entropy dominates over the hydrogen pairing energy. Single, unpaired chemisorbed H atoms be-

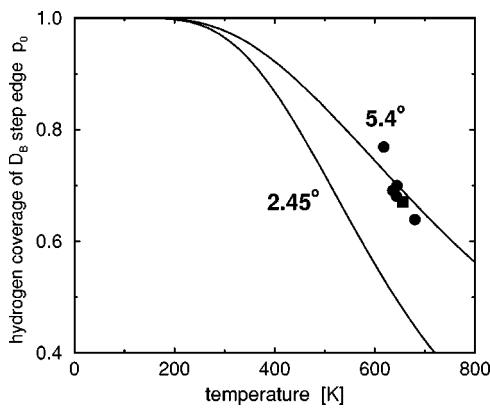


FIG. 8. Same as Fig. 7. However, in this case only partial thermal equilibration of the system is assumed: The adsorbed hydrogen atoms are allowed to diffuse only along the dimer row on a single terrace, or to hop from one Si atom to the other Si atom within the same dimer. Results are based on the Hamiltonian in Eq. (2) and a canonical ensemble. The symbols denote experimental data by Raschke and Höfer for vicinal surfaces with a miscut angle of 2.5° (circles) and 5.5° (square).

come more and more frequent at low H coverage. To account for this process we generalize our model Hamiltonian. The occupation numbers n_i^A and n_i^B can take the values 0 or 1, depending on whether the Si atom A or B of the i th Si surface dimer is H saturated or not. For simplicity we omit the interaction between H atoms on different dimers, i.e., we set all w_i to zero. Furthermore we assume a site-independent pairing energy ϵ_{pair} of 0.25 eV, in agreement with previous experimental and theoretical work for the flat surface.^{17,51} The Hamiltonian is

$$H^{(D_B)} = \sum_{i=0}^N \left\{ \frac{1}{2} (n_i^A + n_i^B) \epsilon_i^{(D_B)} + \frac{1}{2} [n_i^A (1 - n_i^B) + n_i^B (1 - n_i^A)] \epsilon_{\text{pair}} \right\}. \quad (2)$$

We have calculated the H-occupation probability at the D_B step edge, $p_0 = \langle n_0^A + n_0^B \rangle / 2$ for this model. The results are plotted as full lines in Fig. 7. Among the model Hamiltonians discussed above we expect this approach to yield the most realistic description of the Si surface in thermodynamic equilibrium at low H coverage. Theory and experiment agree with respect to the fact that the hydrogen more tightly binds to the step edge than on the terrace. In view of the experimental uncertainty the experimental data are still compatible with the predicted variation of step-edge H coverage with miscut. However, as can be read from Fig. 7, there remains a slight quantitative discrepancy. Because the chemisorption energies at the D_B and at the S_B step edge are similar, we do not attribute this difference to the existence of single atomic height steps on the experimental sample. Instead, we argue that at least part of the difference may be due to the incomplete thermal equilibration of the surface in experiment. There is qualitative agreement between theory⁶⁶⁻⁶⁸ and experiment⁶⁹ that the diffusion of hydrogen atoms on the Si(001) surface is highly anisotropic and fast along the dimer rows. The experimental⁶⁹ activation energy for hopping along a dimer row amounts to $E_B=1.68$ eV when an attempt frequency of $\nu_0=10^{13} \text{ s}^{-1}$ is assumed. At a surface temperature of $T=620$ K this corresponds to a hopping rate $\nu = \nu_0 \exp(-E_B/k_B T) = 0.2 \text{ s}^{-1}$, i.e., many of these diffusion events occur during the time interval of the order of 10^3 s during which the surface is kept at elevated temperature in the Höfer and Raschke experiment. Similarly, the intradimer hopping is predicted to be as fast as the intrarow hopping of the hydrogen atoms.⁶⁶ Thus we may safely assume a perfect thermal scrambling of the H-atom adsorption sites within a single dimer row. The hydrogen interrow diffusion, on the other hand, is distinctly slower. The theoretical barriers vary from 1.8 eV,⁶⁶ which translates into a hopping rate of roughly 0.02 s^{-1} , to barriers much larger than 2 eV,^{67,68} where hopping perpendicular to the dimer rows would be almost completely suppressed. To explore the consequences of partial equilibration we study the limiting case that also the energy barrier for an H atom to cross the step and diffuse onto a neighboring terrace is large, and calculate the thermal expectation value $\langle n_0^A + n_0^B \rangle / 2$ for the hydrogen coverage at the step edge from the Hamiltonian (2) within the canonical ensemble. In this ensemble the number of hydrogen atoms on every single dimer string is restricted to be equal to 2. Indeed the result in Fig. 8 shows a better agreement with

Raschke and Höfer's experiment than Fig. 7, i.e., our calculations are consistent with the notion that at 620–680 K the hopping of H atoms across the row and the exchange of H atoms between rows on different terraces is a rare process within a typical experimental time interval of 10^2 – 10^3 s.

IV. SUMMARY AND CONCLUSIONS

The chemisorption energies for H_2 on vicinal Si(001) surfaces have been calculated using a well-established *ab initio* total-energy technique.⁴⁰ The various adsorption sites on the terraces and at the step edges have been compared to each other. Both the single atomic height S_A - S_B steps and the rebonded and nonrebonded double atomic height D_B and D'_B steps have been considered. The results confirm recent experimental findings by Raschke and Höfer³³ for the adsorption of molecular hydrogen on vicinal Si surfaces.

In particular, we conclude the following from our calculations: (i) On a surface with D_B steps hydrogen preferentially binds to the step-edge Si atoms. The chemisorption energy difference with respect to the terrace sites is ≥ 0.12 eV per H_2 molecule. For adsorption on a Si dimer in the middle of a large (001) terrace the difference amounts to about 0.17 eV per H_2 molecule. (ii) Adsorption on a vicinal surface with single atomic height steps is similar to adsorption on the D_B stepped surface. The hydrogen atoms preferentially bind to the S_B step edge, with nearly the same

chemisorption energy as for the D_B step edge. (iii) The nonrebonded D'_B step, which is known to be unstable on the clean surface,^{37,39} remains unstable also after hydrogen adsorption. (iv) The interaction between neighboring monohydride groups on the Si surface has been calculated and was found to be locally attractive. However, this interaction is too weak to be of importance for the conclusions drawn in this paper. (v) The hydrogen coverage of the D_B step edge has been calculated as function of temperature. We assume that the diffusing hydrogen atoms are confined to a single dimer row and obtain qualitative and within the theoretical and experimental error margins even quantitative agreement with the experiment.³³

This work supplies the basis for a theoretical investigation of the H_2 adsorption energy barriers on vicinal Si(001) surfaces, especially for a comparison between the dissociative adsorption at the step edge and on the Si dimers of the terrace.

ACKNOWLEDGMENTS

We are grateful to M. Scheffler for his continuous support of this work and thank him, W. Brenig, U. Höfer, and M. Raschke for enlightening discussions. This work was supported in part by the Sfb 338 of the Deutsche Forschungsgemeinschaft.

- ¹J. E. Vasek, Z. Zhang, C. T. Salling, and M. G. Lagally, *Phys. Rev. B* **51**, 17 207 (1995).
- ²J. H. G. Owen, K. Miki, D. R. Bowler, C. M. Goringe, I. Goldfarb, and G. A. D. Briggs, *Surf. Sci.* **394**, 79 (1997).
- ³J. H. G. Owen, K. Miki, D. R. Bowler, C. M. Goringe, I. Goldfarb, and G. A. D. Briggs, *Surf. Sci.* **394**, 91 (1997).
- ⁴R. J. Hamers, U. K. Köhler, and J. E. Demuth, *Ultramicroscopy* **31**, 10 (1989).
- ⁵Y. W. Mo, R. Kariotis, B. S. Swartzentruber, M. B. Webb, and M. G. Lagally, *J. Vac. Sci. Technol. B* **8**, 232 (1990).
- ⁶S. Clarke, M. R. Wilby, D. D. Vvedensky, T. Kawamura, K. Miki, and H. Tokumoto, *Phys. Rev. B* **41**, 10 198 (1990).
- ⁷M. Lagally, *Phys. Today* **46**(11), 24 (1993).
- ⁸F. Liu and M. G. Lagally, *Chem. Phys. Solid Surf.* **8**, 258 (1997).
- ⁹O. L. Alerhand, D. Vanderbilt, R. D. Meade, and J. D. Joannopoulos, *Phys. Rev. Lett.* **61**, 1973 (1988).
- ¹⁰O. L. Alerhand, A. N. Berker, J. D. Joannopoulos, D. Vanderbilt, R. J. Hamers, and J. E. Demuth, *Phys. Rev. Lett.* **64**, 2406 (1990).
- ¹¹R. M. Tromp and M. C. Reuter, *Phys. Rev. Lett.* **68**, 820 (1992).
- ¹²M. Horn-von Hoegen and A. Golla, *Phys. Rev. Lett.* **76**, 2953 (1996).
- ¹³K. W. Kolasinski, W. Nessler, A. de Meijere, and E. Hasselbrink, *Phys. Rev. Lett.* **72**, 1356 (1994).
- ¹⁴P. Bratu, K. L. Kompa, and U. Höfer, *Chem. Phys. Lett.* **251**, 1 (1996).
- ¹⁵W. Brenig, A. Groß, and R. Russ, *Z. Phys. B* **96**, 231 (1994).
- ¹⁶P. Bratu, W. Brenig, A. Groß, M. Hartmann, U. Höfer, P. Kratzer, and R. Russ, *Phys. Rev. B* **54**, 5978 (1996).
- ¹⁷U. Höfer, Leping Li, and T. F. Heinz, *Phys. Rev. B* **45**, 9485 (1992).
- ¹⁸C. J. Wu and E. A. Carter, *Chem. Phys. Lett.* **185**, 172 (1991).
- ¹⁹C. J. Wu, I. V. Ionova, and E. A. Carter, *Surf. Sci.* **295**, 64 (1993).
- ²⁰Z. Jing and J. L. Whitten, *J. Chem. Phys.* **98**, 7466 (1993).
- ²¹P. Nachtigall, K. D. Jordan, A. Smith, and H. Jónsson, *J. Chem. Phys.* **104**, 148 (1996).
- ²²P. Kratzer, B. Hammer, and J. K. Nørskov, *Chem. Phys. Lett.* **229**, 645 (1994).
- ²³E. Pehlke and M. Scheffler, *Phys. Rev. Lett.* **74**, 952 (1995).
- ²⁴A. Vittadini and A. Selloni, *Chem. Phys. Lett.* **235**, 334 (1995).
- ²⁵Z. Jing, G. Lucovsky, and J. L. Whitten, *Surf. Sci. Lett.* **296**, L33 (1993).
- ²⁶P. Nachtigall, K. D. Jordan, and C. Sosa, *J. Chem. Phys.* **101**, 8073 (1994).
- ²⁷M. R. Radeke and E. A. Carter, *Phys. Rev. B* **54**, 11 803 (1996).
- ²⁸M. R. Radeke and E. Carter, *Phys. Rev. B* **55**, 4649 (1997).
- ²⁹S. Pai and D. Doren, *J. Chem. Phys.* **103**, 1232 (1995).
- ³⁰M. B. Raschke and U. Höfer, *Appl. Phys. B* (to be published).
- ³¹C. C. Umbach, M. E. Keeffe, and J. M. Blakely, *J. Vac. Sci. Technol. B* **9**, 721 (1991).
- ³²P. Kratzer, E. Pehlke, M. Scheffler, M. B. Raschke, and U. Höfer, *Phys. Rev. Lett.* **81**, 5596 (1998).
- ³³M. B. Raschke and U. Höfer, preceding paper, *Phys. Rev. B* **59**, 2783 (1999).
- ³⁴P. E. Wierenga, J. A. Kubby, and J. E. Griffith, *Phys. Rev. Lett.* **59**, 2169 (1987).
- ³⁵J. E. Griffith, G. P. Kochanski, J. A. Kubby, and P. E. Wierenga,

- J. Vac. Sci. Technol. A **7**, 1914 (1989).
- ³⁶B. S. Swartzentruber, Y.-W. Mo, R. Kariotis, M. G. Lagally, and M. B. Webb, Phys. Rev. Lett. **65**, 1913 (1990).
- ³⁷D. J. Chadi, Phys. Rev. Lett. **59**, 1691 (1987).
- ³⁸P. Bogusławski, Q.-M. Zhang, Z. Zhang, and J. Bernholc, Phys. Rev. Lett. **72**, 3694 (1994).
- ³⁹A. Oshiyama, Phys. Rev. Lett. **74**, 130 (1995).
- ⁴⁰M. Bockstedte, A. Kley, J. Neugebauer, and M. Scheffler, Comput. Phys. Commun. **107**, 187 (1997). See also <http://www.fhi-berlin.mpg.de/th/fhi96md/code.html>.
- ⁴¹J. P. Perdew, J. A. Chevary, S. H. Vosko, K. A. Jackson, M. R. Pederson, D. J. Singh, and C. Fiolhais, Phys. Rev. B **46**, 6671 (1992).
- ⁴²B. Hammer, M. Scheffler, K. W. Jacobsen, and J. Nørskov, Phys. Rev. Lett. **73**, 1400 (1994).
- ⁴³N. Moll, M. Bockstedte, M. Fuchs, E. Pehlke, and M. Scheffler, Phys. Rev. B **52**, 2550 (1995).
- ⁴⁴D. R. Hamann, Phys. Rev. B **40**, 2980 (1989).
- ⁴⁵M. Fuchs and M. Scheffler (unpublished).
- ⁴⁶M. Fuchs, M. Bockstedte, E. Pehlke, and M. Scheffler, Phys. Rev. B **57**, 2134 (1998).
- ⁴⁷H. J. Monkhorst and J. D. Pack, Phys. Rev. B **13**, 5188 (1976).
- ⁴⁸T. W. Poon, S. Yip, P. S. Ho, and F. F. Abraham, Phys. Rev. B **45**, 3521 (1992).
- ⁴⁹F. Stucki, J. A. Schaefer, J. R. Anderson, G. J. Lapeyre, and W. Göpel, Solid State Commun. **47**, 795 (1983).
- ⁵⁰G. P. Kochanski, Phys. Rev. B **41**, 12 334 (1990).
- ⁵¹J. E. Northrup, Phys. Rev. B **51**, 2218 (1995).
- ⁵²R. E. Schlier and H. E. Farnsworth, J. Chem. Phys. **30**, 917 (1959).
- ⁵³D. J. Chadi, Phys. Rev. Lett. **43**, 43 (1979).
- ⁵⁴J. Dąbrowski and M. Scheffler, Appl. Surf. Sci. **56-58**, 15 (1992).
- ⁵⁵R. A. Wolkow, Phys. Rev. Lett. **68**, 2636 (1992).
- ⁵⁶A. I. Shkrebtii, Phys. Rev. Lett. **70**, 2645 (1993).
- ⁵⁷E. L. Bullock, R. Gunnella, L. Patthey, T. Abukawa, S. Kono, C. R. Natoli, and L. S. O. Johansson, Phys. Rev. Lett. **74**, 2756 (1995).
- ⁵⁸H. Over, J. Wasserfall, W. Ranke, C. Ambiatello, R. Sawitzki, D. Wolf, and W. Moritz, Phys. Rev. B **55**, 4731 (1997).
- ⁵⁹J. E. Northrup, Phys. Rev. B **47**, 10 032 (1993).
- ⁶⁰A. Ramstad, G. Brocks, and P. J. Kelly, Phys. Rev. B **51**, 14 504 (1995).
- ⁶¹P. Krüger and J. Pollmann, Phys. Rev. Lett. **74**, 1155 (1995).
- ⁶²X. Tong and P. A. Bennett, Phys. Rev. Lett. **67**, 101 (1991).
- ⁶³E. Pehlke and J. Tersoff, Phys. Rev. Lett. **67**, 1290 (1991).
- ⁶⁴J. J. de Miguel, C. E. Aumann, S. G. Jaloviar, R. Kariotis, and M. G. Lagally, Phys. Rev. B **46**, 10 257 (1992).
- ⁶⁵For this estimate we use the Hamiltonian Eq. (1) and approximate the H₂ chemisorption energy by $[\epsilon_0(D'_B) + \epsilon_1(D'_B) + w_0(D'_B)]/2$.
- ⁶⁶A. Vittadini, A. Selloni, and M. Casarin, Surf. Sci. Lett. **289**, L625 (1993).
- ⁶⁷C. J. Wu, I. V. Ionova, and E. A. Carter, Phys. Rev. B **49**, 13 488 (1994).
- ⁶⁸P. Nachtigall and K. D. Jordan, J. Chem. Phys. **102**, 8249 (1995).
- ⁶⁹J. H. G. Owen, D. R. Bowler, C. M. Goringe, K. Miki, and G. A. D. Briggs, Phys. Rev. B **54**, 14 153 (1996).